Electronic Supplementary Material (ESI) for Sustainable Energy & Fuels.
This journal is © The Royal Society of Chemistry 2017

Supporting Information

Template-free Synthesis of Mesoporous Manganese Oxides with Catalytic Activity in the Oxygen Evolution Reaction

Suoyuan Lian[a**], Michelle P. Browne[a**], Carlota Domínguez[a], Serban N. Stamatin[a], Hugo Nolan[a], Georg S. Duesberg[a], Michael E.G. Lyons[a], Emiliano Fonda[b] and Paula E. Colavita[a*].

[a] School of Chemistry CRANN and AMBER Research Centres, Trinity College Dublin, College Green, Dublin 2, Ireland

[b] Synchrotron SOLEIL L'Orme de Merisiers, St Aubin BP48, 91192 Gif sur Yvette Cedex, France

* Corresponding: Colavitp@tcd.ie

** Joint first author

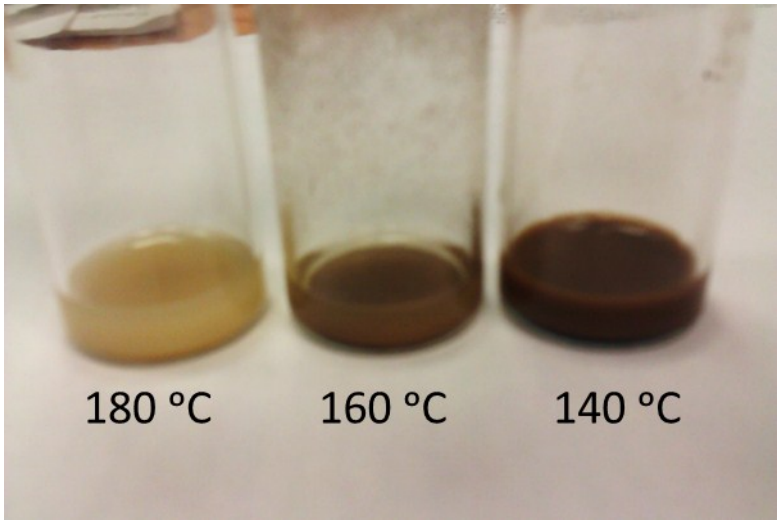

Figure S1. From left to right are the $MnCO_3$ prepared at 180, 160 and 140°C.

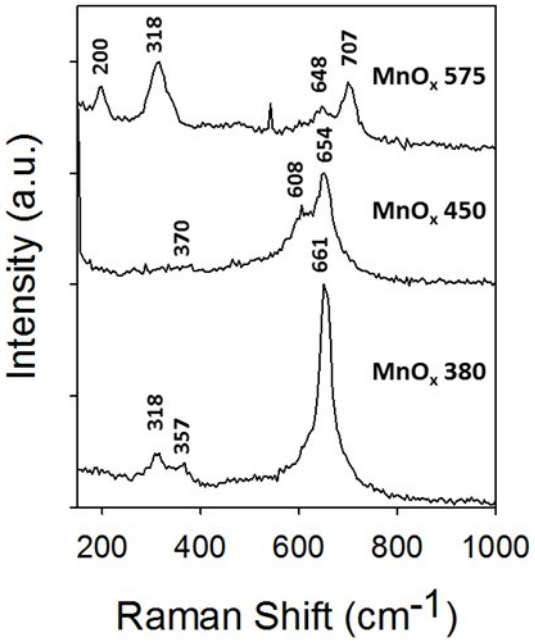

Figure S2. Raman Analysis of samples obtained after annealing at 380, 450 and 575 °C.

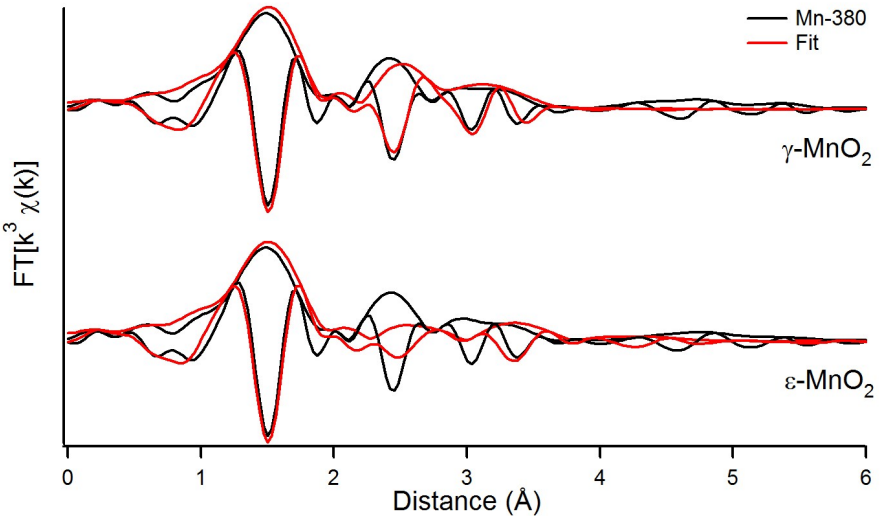

Figure S3. EXAFS fitting of Mn-380 obtained by including the Mn nearest neighbors of γ-MnO_2 (top), or of ε-MnO_2 (bottom) and using single scattering paths up to 4 Å; both modulus and imaginary parts of the Fourier Transforms are reported. It is evident from this comparison that the ε-MnO_2 structure is a poorer match for Mn-380 samples. A comparison of the goodness-of-fit for the two models confirms the conclusions drawn from a graphical comparison, as the ratio of reduced chi-squares for the two models yields χ_ν^2(ε-MnO_2)/ χ_ν^2(γ -MnO_2) = 1.6, thus indicating that the fit is significantly worse for the ε-MnO_2 model.

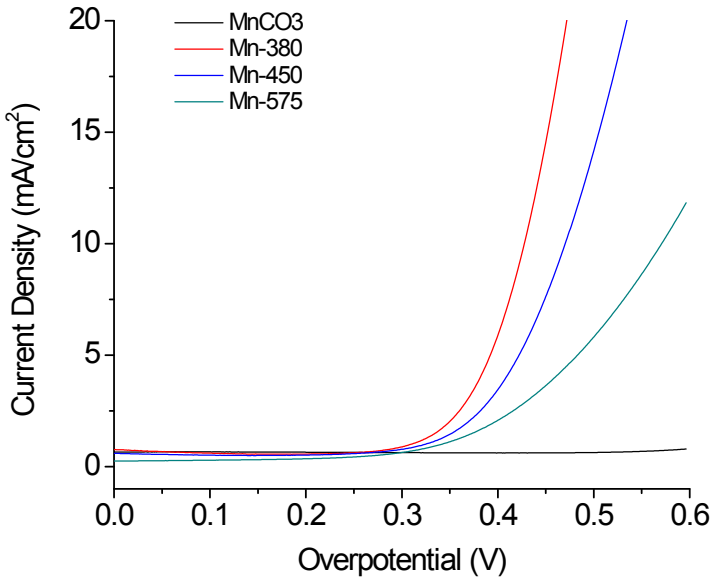

Figure S4. LSVs for all the Mn oxides and solvothermally prepared $MnCO_3$ with respect to overpotential; data obtained in 1 M NaOH at 5 mV s^{-1} with a loading of 1 mg cm^{-2}.

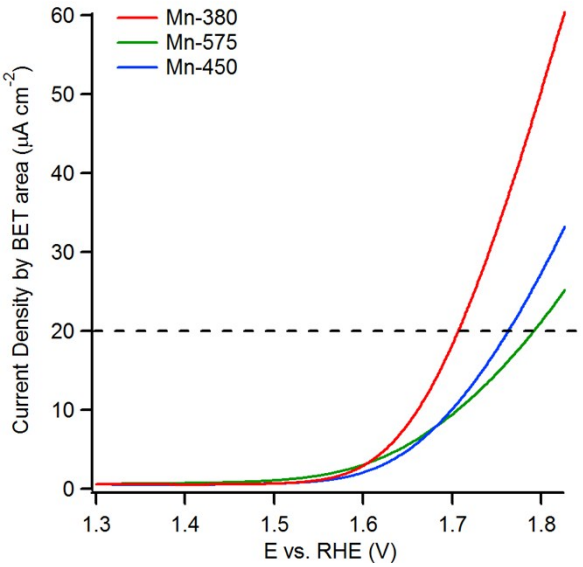

Figure S5. LSVs for the Mn oxides after normalization by the BET area of each material (as opposed to the geometric area); this type of normalization assumes that all N_2-accessible area is also accessible to the electrolyte. The curves indicate that Mn-380 displays the highest activity.

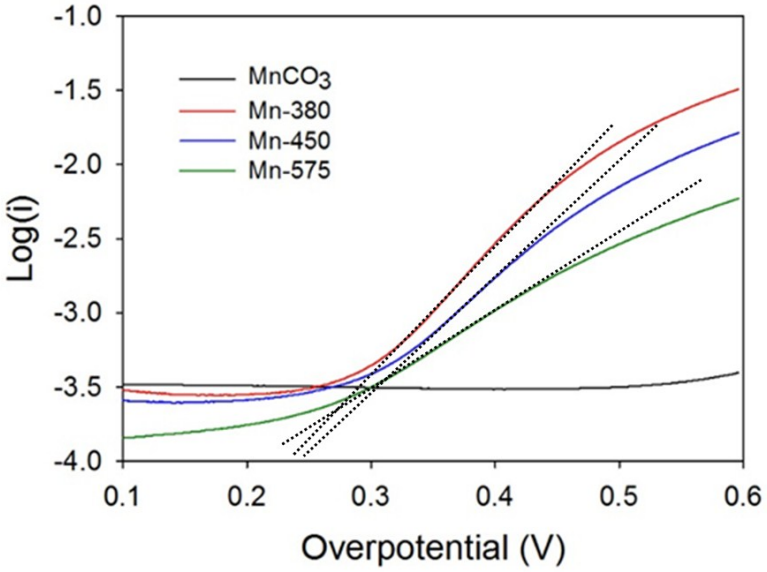

Figure S6. Tafel plots for all the Mn oxides and $MnCO_3$ with respect to overpotential; data obtained in 1 M NaOH at 5 mV s^{-1}. Black dotted line indicates linear region where the Tafel slope was determined from.

Table S1. Tafel slope calculations for OER active samples based on data in Figure S5.

Sample	Tafel slope (mV dec^{-1})
Mn-380	120
Mn-450	130
Mn-575	157

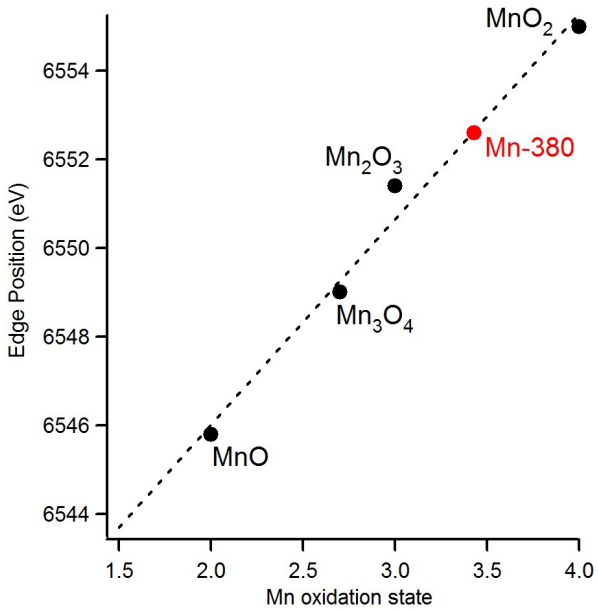

Figure S7. Plot of edge position vs. oxidation state for manganese oxide reference samples (•) used in our experiments. The edge position was determined as the energy at half the normalised edge absorbance. The dashed line shows the best linear fit of the four reference values that was used to interpolate the oxidation state of Mn-380 (•). An accurate determination of oxidation state would require a full principal component analysis as discussed by Manceau et al.(ref. 63 in the main text).

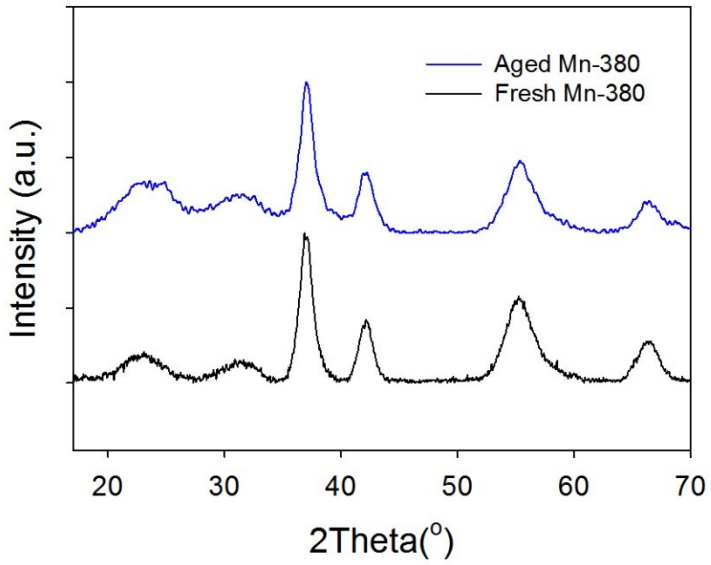

Figure S8. Comparison of the XRD pattern of Mn-380 and Mn-380 after 9 months of ageing in air. Patterns are shown after baseline subtraction and smoothing to facilitate comparison. It is evident that a slow transformation takes place with the appearance of an additional reflection at 26.4° over time. This is consistent with the effects of stress release and Mn(III) migration in defect-rich MnO_2 phases discussed in detail by Grangeon et al.(ref. 67 in the main text).